Fine Structure in the Parameters of Dielectric and Viscoelastic Relaxations

P. A. M. Steeman*,† and J. van Turnhout‡

DSM Research BV, P.O. Box 18, 6160 MD Geleen, The Netherlands, and TNO Plastics and Rubber Institute, P.O. Box 6031, 2600 JA Delft, The Netherlands

Received April 21, 1994; Revised Manuscript Received June 23, 1994®

ABSTRACT: A new method for the analysis of dielectric or viscoelastic data, the calculation of the fine structure in relaxation parameters, is described. The dielectric case is worked out in detail. Use is made of the partial derivatives of the dielectric constant with respect to temperature and frequency. It is shown how the fine structure in activation energy and frequency factor (Arrhenius) or, equivalently, the fine structure in activation enthalpy and activation entropy (Eyring) can be extracted from the data using these derivatives. Results of simulations using a Cole–Cole distribution in frequency factors and a Gaussian distribution in activation energies are discussed. The values of both relaxation parameters are accurately deconvoluted with the fine-structure method. Finally, some experimental results for rigid poly(vinyl chloride) are presented. The typical behavior at the α- and β-transitions is discussed. An additional effect is observed at temperatures close to the α-transition or the structural transition from the glassy to the rubbery state. This effect offers an interesting tool for a nearly frequency-independent assessment of the glass–rubber transition.

Introduction

Polymeric materials are well-known to exhibit very broad, non-Debye-like, relaxation processes. Many attempts have been made to describe these broad transitions empirically and theoretically. A number of empirical equations have been proposed.[1] Those of Cole–Cole,[2] Cole–Davidson,[3] and Havriliak–Negami[4] are used most often for a data analysis in the frequency domain. In the time domain—and among theoreticians—the empirical KWW equation[5–7] is the most popular.

The peak broadening described by these equations is often thought to be due to a distribution of relaxation times present in the material, in contrast to the single relaxation time supposed for the Debye process. Several authors (refs 8 and 9 and references therein) have discussed the physical mechanisms which cause this type of distribution to occur in materials, especially in the solid state. In the case of dipolar polarization this distribution is thought to be due to inter- and intramolecular dipole–dipole[8] or many-body interactions.[10] In the case of a macroscopic or interfacial polarization morphological irregularities as well as inter- and intracluster polarizations[11] play an important role.

Starkweather, assuming an Eyring behavior, has discussed that a distribution in relaxation times may be due to a distribution in activation enthalpies, a distribution in activation entropies, or both.[12,13] He has shown how the distribution in one of these parameters can be extracted from the experimental data when the other parameter is fixed. However, he was not able to extract a simultaneous distribution in both parameters.

In this paper we introduce a method for revealing the so-called fine structure in relaxation parameters. This fine structure depicts both the energy of activation (enthalpic effect) and the frequency factor (entropic effect) of the polarizable entities contributing at any given temperature and frequency to the observed relaxation processes. In contrast to the traditional analysis, in which only the frequencies of maximum loss are collected and analyzed as a function of temperature, the fine-structure method uses the full scale of the experimental data available. This novel analysis method is illustrated with some theoretical simulations. First, a distribution in frequency factor with constant activation energy and, second, a distribution in activation energy with constant frequency factor are considered. Finally, some experimental results on poly(vinyl chloride) are presented.

Theory

In the following the theory of the extraction of the fine structure in relaxation parameters will be worked out in detail for the dielectric case. However, an analogous derivation can be made for the viscoelastic case after replacing the dielectric constant ϵ' in the formulas by the storage modulus (E', G') or the storage compliance (B', J').

In performing dynamic dielectric measurements the dynamic response of the material is investigated. In the frequency range studied (mHz to MHz), the atomic and electronic polarization mechanisms react instantaneously, while the dipolar and macroscopic mechanisms need some time to build up a polarization. The instantaneous polarization raises the dielectric constant to a level of ϵ_∞. The dynamic response of the system is related to the $i\omega$ Laplace transform of the impulse response of the slower noninstantaneous mechanisms f_p through[1]

$$\epsilon^*(\omega) = \epsilon_\infty + (\epsilon_s - \epsilon_\infty)\, L_{i\omega}(f_p) \tag{1}$$

in which ϵ_s and ϵ_∞ are the static and high-frequency limiting values of the dielectric constant, respectively.

For a single-relaxation process with an exponential decay function and relaxation time τ, a Debye type response is obtained:

$$\epsilon^*(\omega) = \epsilon_\infty + \frac{\epsilon_s - \epsilon_\infty}{1 + i\omega\tau} \tag{2}$$

In many cases, however, the material shows a more complex behavior and a distribution of relaxation times is present. In that case relation 2 is generalized by invoking a logarithmic distribution of the relaxation times $g(\ln \tau)$:

* To whom correspondence should be addressed.
† DSM Research BV.
‡ TNO Plastics and Rubber Institute.
® Abstract published in *Advance ACS Abstracts*, August 1, 1994.

0024-9297/94/2227-5421$04.50/0

$$\epsilon^*(\omega) = \epsilon_\infty + (\epsilon_s - \epsilon_\infty)\int_{-\infty}^{\infty} \frac{g(\ln \tau)}{1 + i\omega\tau}\, d(\ln \tau) \quad (3)$$

The real and the imaginary parts of this equation yield the relations for the dielectric constant ϵ' and the loss index ϵ'':

$$\epsilon'(\omega) = \epsilon_\infty + (\epsilon_s - \epsilon_\infty)\int_{-\infty}^{\infty} \frac{g(\ln \tau)}{1 + \omega^2\tau^2}\, d(\ln \tau) \quad (4)$$

$$\epsilon''(\omega) = (\epsilon_s - \epsilon_\infty)\int_{-\infty}^{\infty} \frac{\omega\tau\, g(\ln \tau)}{1 + \omega^2\tau^2}\, d(\ln \tau) \quad (5)$$

The relaxation time τ of the polarization process depends on the temperature T. This temperature dependence can often be described by the well-known Arrhenius relation:[14]

$$\tau(T) = \tau_\infty \exp(E_{act}/RT) \quad (6)$$

in which τ_∞ (s) and E_{act} (J mol^{-1}) are constants, called the frequency factor (relaxation time at infinite temperature) and the activation energy of the polarization mechanism, respectively. R is the gas constant (8.314 J mol^{-1} K^{-1}) and T (K) is the absolute temperature.

From relation 6 it can be deduced that three underlying effects may cause a distribution in relaxation times:

1. A distribution in τ_∞ values with only one activation energy, in which case the material shows a rheologically simple behavior. The distribution of relaxation times is independent of temperature.
2. A distribution in activation energies E_{act} with only one τ_∞ value. The distribution of relaxation times now depends on temperature and tends to become narrower with increasing temperature.
3. A distribution in both activation energies and τ_∞ values. Often the material behaves according to the compensation law,[15,16] which implies that a linear relation between τ_∞ and E_{act} exists for subrelaxations belonging to one relaxation mechanism.

In general, a two-dimensional distribution function $f(E_{act}, \ln \tau_\infty)$, which is independent of temperature, should therefore be used to describe the relaxation time spectrum.

From eqs 4 and 6 the derivatives of the dielectric constant with respect to frequency and temperature can be calculated. Using a two-dimensional distribution function and neglecting the (limited) temperature dependence of ϵ_s and ϵ_∞, the following result is obtained:

$$\frac{1}{\epsilon_s - \epsilon_\infty}\partial\epsilon'/\partial(1/T) = \int_0^\infty\int_{-\infty}^{\infty} \partial/\partial(1/T)\left(\frac{1}{1 + \omega^2\tau^2}\right) \times f(E_{act}, \ln \tau_\infty)\, dE_{act}\, d(\ln \tau_\infty) \quad (7)$$

$$= \int_0^\infty\int_{-\infty}^{\infty} (E_{act}/R)\frac{-2\omega^2\tau^2}{(1 + \omega^2\tau^2)^2} \times f(E_{act}, \ln \tau_\infty)\, dE_{act}\, d(\ln \tau_\infty) \quad (8)$$

and

$$\frac{1}{\epsilon_s - \epsilon_\infty}\partial\epsilon'/\partial(\ln \omega) = \int_0^\infty\int_{-\infty}^{\infty} \omega\, \partial/\partial\omega\left(\frac{1}{1 + \omega^2\tau^2}\right) \times f(E_{act}, \ln \tau_\infty)\, dE_{act}\, d(\ln \tau_\infty) \quad (9)$$

$$= \int_0^\infty\int_{-\infty}^{\infty} \frac{-2\omega^2\tau^2}{(1 + \omega^2\tau^2)^2} f(E_{act}, \ln \tau_\infty) \times dE_{act}\, d(\ln \tau_\infty) \quad (10)$$

The first terms in the integral kernels of eqs 8 and 10 are equal. This term, $h_1(\omega\tau) = 2\omega^2\tau^2/(1 + \omega^2\tau^2)^2$, is an intensity function which shows a sharp peak around $\omega = 1/\tau$.

Because of the sharpness of this intensity function at $\omega = 1/\tau$, it is allowed to approximate the integral relations (8) and (10) by evaluating them at $\tau = 1/\omega$ only (see Appendix). The relations then reduce to

$$\frac{1}{\epsilon_s - \epsilon_\infty}\partial\epsilon'/\partial(1/T) \approx -\int_0^\infty (E_{act}/R) \times f(E_{act}, -\ln \omega - E_{act}/RT)\, dE_{act} \quad (11)$$

$$\approx (-1/R)E_{act}|_{\omega\tau=1}\int_0^\infty f(E_{act}, -\ln \omega - E_{act}/RT)\, dE_{act}$$

$$\approx (-1/R)E_{act}|_{\omega\tau=1}\, g(\ln \tau)_{\tau=1/\omega}$$

and

$$\frac{1}{\epsilon_s - \epsilon_\infty}\partial\epsilon'/\partial(\ln \omega) \approx -\int_0^\infty f(E_{act}, -\ln \omega - E_{act}/RT)\, dE_{act} = -g(\ln \tau)|_{\tau=1/\omega} \quad (12)$$

in which $E_{act}|_{\omega\tau=1}$ is the weighted average of the activation energies of all processes with a relaxation time $\tau = 1/\omega$ at temperature T.

In eq 5 for the dielectric loss index ϵ'', too, an intensity function is contained in the integration kernel. This intensity function $h_2(\omega\tau) = (2/\pi)\omega\tau/(1 + \omega^2\tau^2)$ also peaks at $\omega = 1/\tau$, though it is less sharp than the previously discussed one. As was discussed for the derivatives of ϵ', relation 5 can be approximated by

$$\epsilon''(\omega) \approx (\epsilon_s - \epsilon_\infty)(\pi/2)\, g(\ln \tau)|_{\tau=1/\omega} \quad (13)$$

By combining eqs 11 and 12 with eq 13, two approximations for calculating the dielectric loss index ϵ'' from the temperature and frequency dependence of the dielectric constant ϵ' are obtained:

$$\epsilon''(\omega) \approx -(\pi/2)\, \partial\epsilon'/\partial(\ln \omega) \quad (14)$$

and

$$\epsilon''(\omega) = -(\pi/2)(R/E_{act})\, \partial\epsilon'/\partial(1/T) \approx (\pi/2)(RT^2/E_{act})\, \partial\epsilon'/\partial T \quad (15)$$

Using these equations, of which the first is well-known,[1] an approximation for calculating the dielectric loss from the polarization part only is obtained. Interestingly, the conduction loss is eliminated in this calculated loss, since electrical conduction mechanisms do not contribute to the dielectric constant of the material. This offers the possibility to study polarization losses even in the liquid or rubbery state of polymers, where the normal loss values are usually overshadowed by the high conduction losses.

Relation 15 contains the activation energy of the polarization process as a parameter. This has two interesting consequences. First, in calculating $\partial\epsilon'/\partial T$, loss peaks from mechanisms with a high activation energy will be enhanced with respect to loss peaks of low activation energy. This implies that peaks due to relaxations of the main chain are accentuated compared to those of the side chains. Second, by taking the ratio of $\partial\epsilon'/\partial(1/T)$ and $\partial\epsilon'/\partial(\ln \omega)$, the *specific activation energy* $E_{act}(\omega,T)$ of the polarization subprocesses giving a maximum loss at an angular frequency ω and at a temperature T can be

calculated from

$$E_{act}(\omega,T)/R = \frac{\partial\epsilon'/\partial(1/T)}{\partial\epsilon'/\partial(\ln\omega)} \quad (16)$$

Using eq 16 the activation energy fine structure of the material can be extracted. The *specific frequency factor* $\tau_\infty(\omega,T)$ of the polarization subprocesses giving a maximum loss at an angular frequency ω and at a temperature T can be calculated from the Arrhenius equation using $\omega = 1/\tau$:

$$\tau_\infty(\omega/T) = (1/\omega)\exp(-E_{act}(\omega,T)/RT) \quad (17)$$

From eq 12 a first estimate of the intensity of the distribution function $g(\ln\tau)$ at $\tau = 1/\omega$ can be obtained, which equals the fraction of the polarization processes with a specific combination of activation energy E_{act} and time constant $\ln\tau_\infty$ yielding a relaxation time τ.

Usually, only the frequencies of maximum dielectric loss and the associated temperatures are used for calculating the Arrhenius activation parameters from eq 6 and $\omega\tau = 1$. With the fine-structure method introduced above, much more detailed information is obtained, including the data at the loss maxima as a small subset.

In this work the derivatives of the experimental ϵ' were calculated using the smoothing filters introduced by Savitzky and Golay[17] and by Gorry[18] or by cubic splines curve fitting.

Simulations

As an example of the results obtained with the fine-structure method, two cases were simulated theoretically: (1) a distribution of $\ln\tau_\infty$ at constant E_{act} and (2) a distribution of E_{act} at constant $\ln\tau_\infty$.

(1) In simulating a distribution of time constants $\ln\tau_\infty$, the symmetrical Cole–Cole distribution was used.[24] According to the Cole–Cole relation, the complex dielectric constant equals[1]

$$\epsilon^*(\omega) = \epsilon_\infty + \frac{\epsilon_s - \epsilon_\infty}{1 + (i\omega\tau_0)^\alpha} = \int_{-\infty}^{\infty}\frac{(\epsilon_s - \epsilon_\infty)\,f(\ln\tau_\infty)}{1 + i\omega\tau_\infty\exp(E_{act}/RT)}\,d(\ln\tau_\infty) \quad (18)$$

in which α, with $0 \le \alpha \le 1$, is the broadening parameter, ϵ_∞ is the high-frequency limit of the dielectric constant, ϵ_s is the low-frequency limit, and τ_0 is the characteristic relaxation time. For a lower α a broader distribution is obtained.

In this simulation a central value $\ln\tau_\infty = -36.5$ and $E_{act} = 60$ kJ/mol^{-1} were assumed. The broadening parameter was set to a practical value of $\alpha = 0.6$, while $\epsilon_s = 2$ and $\epsilon_\infty = 1$.

Figure 1 shows the isochronous dielectric loss curves as a function of temperature at several frequencies between 1 mHz and 1 GHz for 1.5 decade frequency intervals, while in Figure 2 the isothermal curves are plotted as a function of frequency at temperatures between −100 and +250 °C for 50 °C temperature intervals. With increasing frequency the loss peaks become broader along the temperature axis. However, along the frequency axis the loss peak width does not change, which typifies a thermorheologically simple behavior. The height of the loss peaks is independent of the temperature.

From the (numerical) derivatives of ϵ' with respect to $\ln\omega$ and to temperature, the activation energy E_{act} and $\ln\tau_\infty$ fine structure was extracted and plotted in Figures 3 and 4 as a function of temperature. For E_{act} one constant value of 60 kJ mol^{-1}, namely, that used for the simulation,

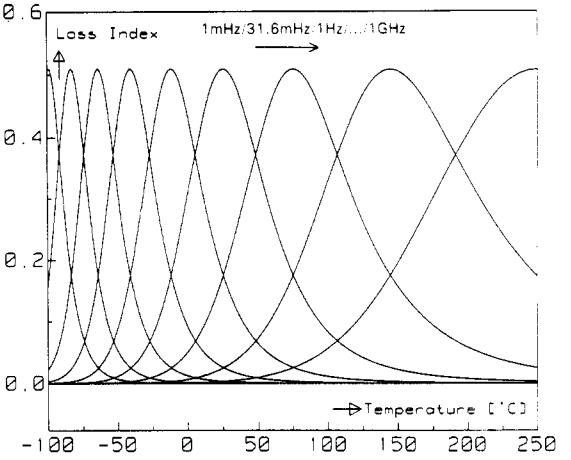

Figure 1. Dielectric loss curves for a Cole–Cole dispersion with $\alpha = 0.6$ as a function of temperature at several frequencies between 1 mHz and 1 GHz.

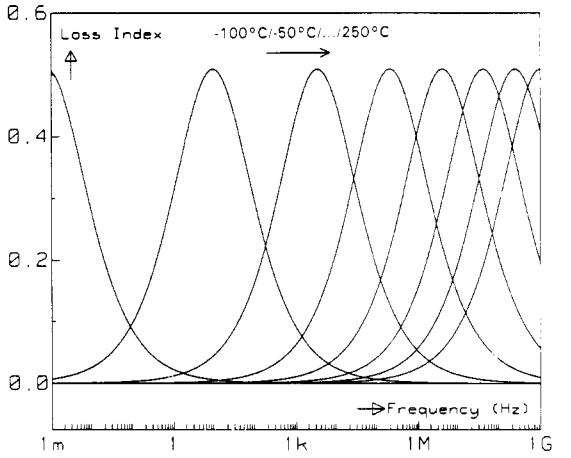

Figure 2. Dielectric loss curves for a Cole–Cole dispersion with $\alpha = 0.6$ as a function of frequency at several temperatures between −100 and +250 °C.

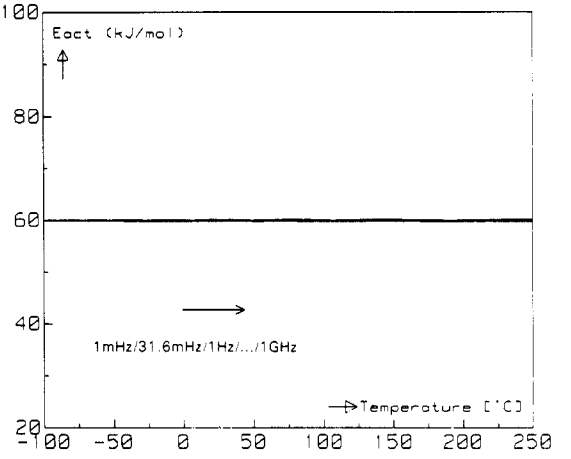

Figure 3. Activation energy fine-structure diagram of the Cole–Cole dispersion studied.

is found over the complete frequency and temperature range studied. At the same time $\ln\tau_\infty$ shows a steady increase with increasing temperature, with a central value of −36.5 at the loss peak maxima. At lower temperatures relaxation mechanisms with lower $\ln\tau_\infty$ are singled out, while at higher temperatures the processes with higher $\ln\tau_\infty$ are found.

These numerical results are in exact agreement with analytical results for this distribution.

(2) In simulating a distribution of activation energies with a constant τ_∞ value a Gaussian distribution was taken.

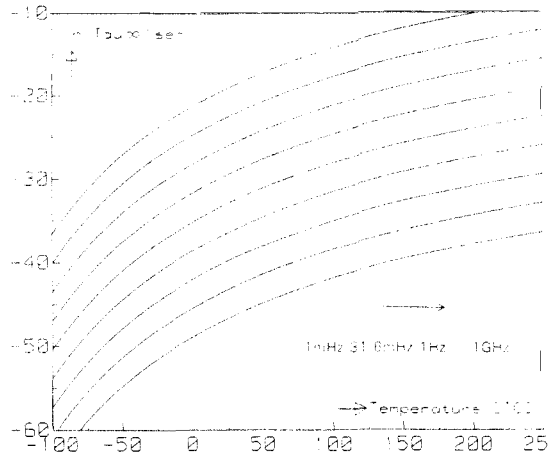

Figure 4. Frequency factor ($\ln \tau_\infty$) fine-structure diagram of the Cole–Cole dispersion studied.

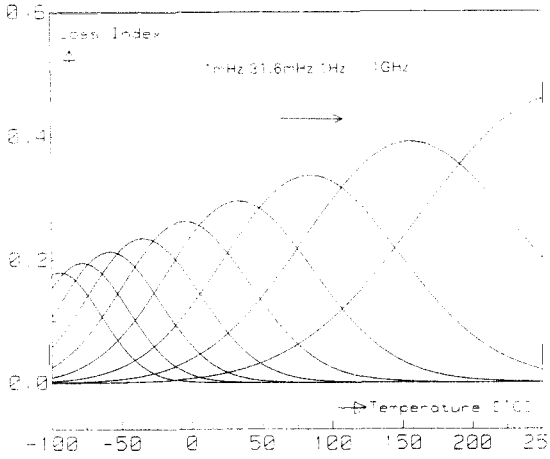

Figure 5. Dielectric loss curves for a Gaussian distribution of activation energies as a function of temperature at several frequencies between 1 mHz and 1 GHz (the parameters are specified in the text).

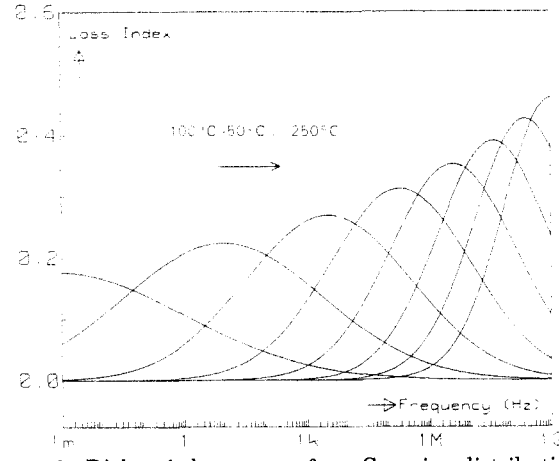

Figure 6. Dielectric loss curves for a Gaussian distribution of activation energies as a function of frequency at several temperatures between −100 and +250 °C (the parameters are specified in the text).

The central activation energy was E_{act} = 60 kJ mol^{-1}, with a standard deviation of 10 kJ mol^{-1}. As in the previous simulation $\ln \tau_\infty$ was set to −36.5. Figure 5 shows the isochronous dielectric loss curves as a function of temperature at several frequencies between 1 mHz and 1 GHz for 1.5 decade frequency intervals, while Figure 6 shows isothermal curves as a function of frequency at temperatures between −100 and +250 °C for 50 °C temperature intervals. The curves were calculated by numerical

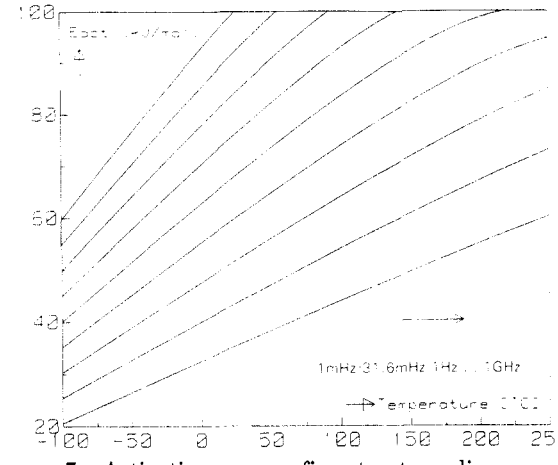

Figure 7. Activation energy fine-structure diagram of the Gaussian distribution studied.

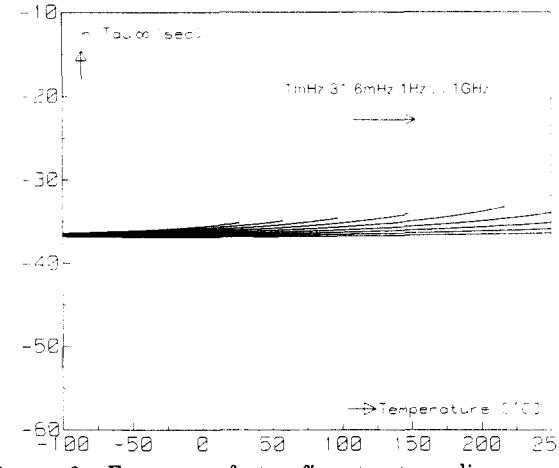

Figure 8. Frequency factor fine-structure diagram of the Gaussian distribution studied.

summation of the subprocesses in the Gaussian distribution. In contrast to the Cole–Cole curves the magnitude of the loss peaks increases markedly with increasing frequency, while the curves become sharper along the frequency axis.

From the derivatives of ϵ' the activation energy E_{act} and $\ln \tau_\infty$ fine structure was obtained and plotted in Figures 7 and 8. A nearly constant $\ln \tau_\infty$ = −36.5 is obtained over the entire temperature and frequency range, with only minor deviations at the extreme loss peak tails; they are probably due to numerical inaccuracy. By contrast, E_{act} varies strongly with frequency and temperature. At the loss peak maxima the central value of 60 kJ mol^{-1} is again found. At lower temperatures the relaxation processes with lower E_{act} values are resolved, while at higher temperatures the processes with higher E_{act} values are found.

Experimental Results

Dielectric measurements were performed on suspension-polymerized PVC (at 44 °C), with M_n = 65 kg mol^{-1} and M_w = 140 kg mol^{-1}, which was kindly supplied by the Limburgse Vinyl Maatschappy (LVM), Tessenderlo, Belgium. Measurements were performed at temperatures between −100 and +130 °C with 1 °C intervals using a set of geometrically spaced measurement frequencies between 0.125 Hz and 65.5 kHz. Measurement of one frequency scan took about 7–8 min for each temperature. A dielectric spectrometer built around a Solartron 1260 frequency response analyzer and interfaced to the sample capacitor with a custom-built electrometer was used.

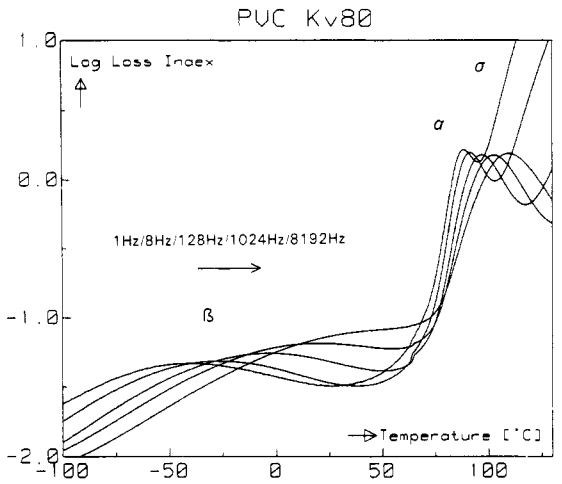

Figure 9. Dielectric loss curves of rigid PVC as a function of temperature at several frequencies between 1 Hz and 8.2 kHz.

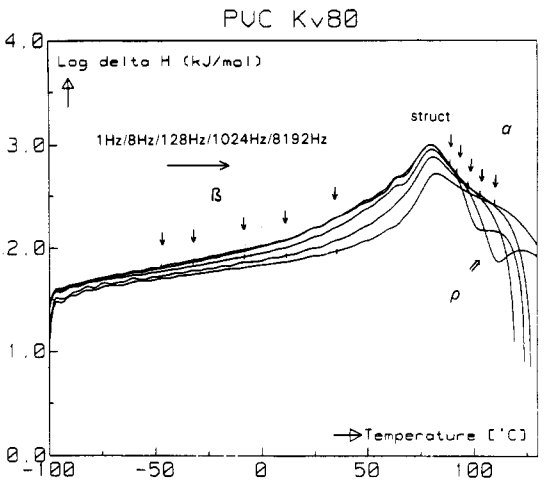

Figure 10. Activation enthalpy fine-structure diagram of the PVC studied as a function of temperature at several frequencies between 1 Hz and 8.2 kHz.

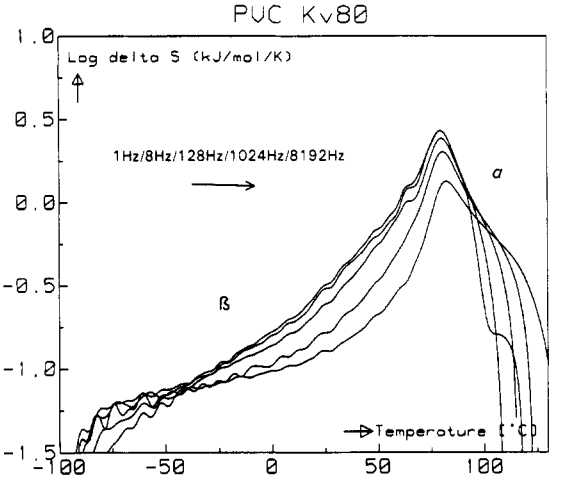

Figure 11. Activation entropy fine-structure diagram of the PVC studied as a function of temperature at several frequencies between 1 Hz and 8.2 kHz.

Figure 9 shows the dielectric loss index measured at 1, 8, 128, 1024, and 8192 Hz as a function of temperature. The broad and weak β-transition is clearly observed at temperatures below 50 °C, while the strong and sharp α-transition (due to the glass–rubber transition) is found at temperatures above 80 °C. Finally, at the highest temperatures and the lowest frequencies the losses increase sharply due to electrical conduction in the rubbery state.

Using the derivatives of the dielectric constant ϵ' (which is not shown here) with respect to the angular frequency and to the temperature, the fine structure in relaxation parameters was extracted.

Following Starkweather,[12,13] the results are expressed in terms of the Eyring equation:

$$\omega = (kT/h) \exp(-\Delta H/RT) \exp(\Delta S/R) \qquad (19)$$

in which ΔH (kJ mol^{-1}) and ΔS (kJ mol^{-1} K^{-1}) are the activation enthalpy and entropy of the transition, h is the Planck constant (6.63×10^{-34} J s), and k is the Boltzmann constant (1.38×10^{-23} J/K).

Starkweather has shown that the activation energy E_{act} in the Arrhenius equation and the activation enthalpy in the Eyring equation are related according to

$$E_{act} = \Delta H + RT \qquad (20)$$

Thus when the specific activation energy $E_{act}(\omega,T)$ is known from eq 16, the specific activation enthalpy $\Delta H(\omega,T)$ can be obtained by subtracting RT. Equivalently, the specific activation entropy $\Delta S(\omega,T)$ can be obtained from

$$\Delta S(\omega,T) = R \ln(h\omega/kT) + \Delta H(\omega,T)/T \qquad (21)$$

Figures 10 and 11 show the activation enthalpy and activation entropy fine structure for the PVC sample studied. Several features can be observed in these figures.

First, in the temperature range of the β-transition activation enthalpies between 30 and 100 kJ mol^{-1} are obtained. The activation entropy is small (<0.1 kJ mol^{-1} K^{-1}), being indicative for a local mechanism of motion in the chain (secondary transition in the glassy state). At the lowest temperatures the lowest activation enthalpies are found, while with increasing temperature higher values are obtained. The activation enthalpy is also distributed along the frequency axis; at the lowest frequencies the highest enthalpies are found. This distribution broadens with increasing temperature, a phenomenon which was also observed in the simulation with the Gaussian distribution of activation energies. At the loss peak maxima (indicated with arrows) an activation enthalpy of about 65 kJ mol^{-1} is obtained for all frequencies, which is about equal to the average value found by fitting the Arrhenius equation to the frequencies and temperatures of maximum loss only.

Second, in the temperature range of the α-transition the activation enthalpy is strongly dependent on both the temperature and the frequency. In fact, a description based on the Doolittle equation, using the free-volume dependence of the relaxation time, would be more appropriate.

Following Saito,[19] the relaxation time τ depends on the free-volume v_f following

$$\tau(T) = \tau_\infty \exp(B/v_f(T)) \qquad (22)$$

For $T > T_g$ the temperature dependence of v_f is given by

$$v_f(T) = v_f(T_g) + \alpha_f(T - T_g) \qquad (23)$$

in which α_f is the thermal expansion coefficient of the free volume and T_g is the glass transition temperature, defined as the temperature at which an increase in the slope of the sample volume versus temperature is observed (dilatometric T_g). Using these two equations, it can be easily derived that

$$\frac{\partial\epsilon'/\partial T}{\partial\epsilon'/\partial(\ln\omega)} = -B\alpha_f/v_f^2(T) \qquad (24)$$

It should be noted that in eq 24 the derivative of the dielectric constant with respect to temperature is used,

while in eq 16 the derivative with respect to the reciprocal temperature is used. Despite the possibility to obtain the free volume parameters, we prefer in this paper to use the apparent activation energies obtained with the Arrhenius relation.

In the temperature range 78–82 °C very high values of the activation enthalpy (up to 1000 kJ mol^{-1}) and entropy are obtained at all frequencies. The loss peak maxima of the α-transition, however, are observed at 10–40 °C higher temperatures. At the α-loss peak maxima enthalpies in the range of 200–400 kJ mol^{-1} are found which decrease sharply with increasing frequency. This behavior is in agreement with the WLF relation (decreasing apparent activation energy with increasing frequency), which is expected to hold at the glass–rubber transition. Meanwhile, activation entropies in the range of 0.3–1 kJ mol^{-1} K^{-1} are found at the loss peak maxima, indicating a highly collective mechanism of motion; they agree well with the values reported by Starkweather.[13]

The high activation enthalpies observed near 80 °C are in close agreement with the values for the apparent activation enthalpy quoted by Saito[19] at the glass transition (>200 kcal mol^{-1}). In this temperature range processes with a very high apparent activation energy during the transition from the glassy to the rubbery state are detected. The relaxation strength of these processes is low. Clearly, owing to the very high enthalpies only a limited shift in temperature with increasing frequency can be expected. However, up to about 100 Hz a nearly identical activation enthalpy is deduced at all frequencies. The decrease at higher frequencies might be due to overlap with the β-relaxation, which causes the calculated (average) enthalpy to be lowered. Probably one common mechanism, being effective at all frequencies simultaneously and active at the glass–rubber transition, causes the observed high activation enthalpies. Since no distinct loss peaks are found, it is most likely coupled to or forms part of the α-relaxation. A possible explanation might be that it is due to the structural relaxation of the material in passing from a nonequilibrium free volume in the glassy state to an equilibrium free volume in the rubbery state. As discussed by Saito, such an effect is expected to occur at temperatures close to the glass–rubber transition. This structural relaxation will have a distinct effect on the α-relaxation at all frequencies simultaneously. Its transition temperature is expected to depend on the thermal history of the sample. Indeed, the peak temperature could be increased by several degrees by annealing the material for 30 min at 80 °C. This is the subject of further investigations. The phenomenon is not specific for PVC. We have observed similar effects in polycarbonate (PC), styrene–acrylonitrile copolymer (SAN), and poly(methyl methacrylate (PMMA). We think that this mechanism enables a more direct assessment of the transition from the glassy to the rubbery state, because the peak temperatures hardly depend on the measuring frequency.

Finally, at the lowest frequencies and the highest temperatures, the activation enthalpy of another, space-charge (ρ) transition in PVC is found. The origin of this space-charge effect, of which the loss peaks are not visible due to the high conduction losses, has recently been discussed in ref 20.

Discussion

The computer simulations represent the two extreme cases which can occur in actual materials: a distributed frequency factor with a constant activation energy and a distributed activation energy with a constant frequency factor. Typical features of the first case, i.e., a distributed frequency factor are as follows:

In isochronal temperature scans the loss peak broadens with increasing frequency.

In isothermal frequency scans, the peak width remains constant.

The peak height is independent of temperature.

The frequency factor increases with temperature, while the activation energy is constant.

In the case of a distributed activation energy the salient features are the following:

The peak height increases with temperature and frequency.

In isothermal frequency scans, the peak sharpens at higher temperatures.

The activation energy increases with temperature and frequency, while the frequency factor is constant. In the case of a combined distribution in both parameters intermediate results are obtained.

In the experimental section the isochronal temperature scans on PVC show (Figure 9) that the peak height of the β-transition increases with increasing frequency. The fine-structure calculations show that the activation enthalpy (Figure 10) is distributed with a constant value at the peak maxima. The activation entropy (Figure 11) of this transition is rather small. All of these characteristics point to the second case simulated, i.e., a constant ln τ_∞ and a distributed E_{act}. This conclusion is consistent with earlier work by Starkweather and co-workers,[13] who observed for a number of secondary relaxations that the distribution of activation free energies is independent of temperature; i.e., the activation entropy for these transitions is close to zero, while the distribution in activation free energies is actually a distribution in activation enthalpies.

For the α-transition the situation seems to be reversed. The peak height is approximately independent of frequency. In isochronal temperature scans the peak broadens with increasing frequency. These results are in line with the characteristics for a relaxation process with a constant activation energy and a distributed frequency factor, i.e., the first case simulated. The activation enthalpy fine structure (Figure 10) does indeed show that the curves for the different frequencies tend to merge in the main part of the loss peaks; thus only a narrow distribution in activation enthalpies is found. However, the activation entropy also shows a limited distribution. Probably both effects cause the observed peak broadening with a predominant role for the distribution in activation entropies. This conclusion agrees well with the results obtained by Starkweather,[13] who has shown that the distribution in activation free energies at the α-transition is temperature dependent and can be due to both a distribution in activation enthalpies and a distribution in activation entropies. However, due to the limited temperature range over which the α-transition is observed, the experimental data did not allow him to distinguish between these two cases. In the present paper it was shown that the fine-structure method does offer this possibility.

At this point a final remark has to be made on the application of the Eyring or Arrhenius equation to the α-relaxation at the glass transition. Originally these equations were developed for chemical reactions. In applying them to viscoelastic and dielectric relaxations, the implicit assumption is made that the underlying process is the same over a range of temperatures. For secondary relaxations like the β-relaxation investigated (localized mechanisms of motion) this assumption probably holds; at the loss peak maxima nearly constant values

for the relaxation parameters are found. For the glass transition the situation is complicated due to the increase of (free) volume with temperature. This causes the amount of material which must move cooperatively to decrease with increasing temperature, which is expected to affect the activation parameters of the process. As modeled by Matsuoka and Quan[21] and experimentally found by Sauer et al.[22] and Starkweather,[23] the activation enthalpy at temperatures above the glass transition decreases with increasing temperature while the activation entropy approaches zero. An analysis of data measured over a large temperature interval (such as an Arrhenius analysis using the loss peak maxima only) is therefore prone to errors. However, the fine-structure method, which is based on derivatives of the dielectric constant with respect to temperature and frequency, delivers the specific values for the activation parameters at a given temperature and should therefore clearly reflect the changes in these parameters with temperature.

In line with these expectations it can be observed in the fine-structure results (Figures 10 and 11) that, after passing the glass transition, both the activation enthalpy and the activation entropy decrease sharply with increasing temperature, in agreement with previous theoretical and experimental observations.[21-23]

Conclusions

The fine-structure method correctly predicts the activation energy and τ_∞ values used in the simulations. It was demonstrated that for a distribution in frequency factors the shape of the loss curves (along the frequency axis) is independent of temperature. By contrast, for a distribution in activation energies the loss curves become narrower with increasing temperature, while the maximum loss increases.

Experimentally, the shape of the dispersion curves often changes with temperature. This is in conflict with the time–temperature superposition principle. The change in shape may be attributed to a change of the broadening parameters describing the empirical relaxation curves. However, these changes cannot easily be related to the underlying physical mechanisms which cause the actual change in curve shape. It was shown that the fine-structure method thus allows a more detailed investigation of the mechanisms causing the peak broadening observed.

Experimental results on poly(vinyl chloride) clearly show the difference in relaxation behavior between secondary transitions in the glassy state and the glass–rubber transition. An Arrhenius and a WLF behavior are observed at the corresponding loss peak maxima, respectively. Evidence for a distribution in activation enthalpies at the β-transition is obtained, which agrees with the observed increase in loss magnitude with increasing frequency. The broadening of the α-transition is probably mainly due to a distribution in activation entropies. An additional mechanism with very high activation enthalpy is found—at all frequencies simultaneously—at temperatures slightly below the α-transition. The present treatment seems a promising tool in assessing the structural transition from the glassy to the rubbery state.

Acknowledgment. The authors wish to thank one of the referees for his detailed comments on the manuscript and his suggestions for improvement.

Appendix: Accuracy of the Integral Approximations

In the derivation of eqs 11 and 12 it was assumed that the integral kernel in eqs 8 and 10 could be replaced by a delta function at $\omega\tau = 1$. For the common experimental (broad) distribution functions this assumption does not introduce a major error. However, for narrow discrete distribution functions the assumption does not hold. In fact, it is easily shown that for a single Debye process the integral (eqs 8 and 10) equals 2 times the square of the dielectric loss.

As an example, for a discrete distribution of activation energies containing merely two activation energies, E_1 and E_2, the activation energy fine structure calculated with eq 16 equals

$$E_{act}(\omega,T) = \frac{\epsilon''_1{}^2 E_1 + \epsilon''_2{}^2 E_2}{\epsilon''_1{}^2 + \epsilon''_2{}^2} \tag{25}$$

in which $\epsilon''_1(\omega,T)$ and $\epsilon''_2(\omega,T)$ are the losses due to the two Debye subprocesses, respectively. At the nonoverlapping loss peak regions the activation energy of the corresponding loss process is extracted, whereas in the region of strong overlap intermediate values are extracted, which are not present in the actual distribution. However, this overlap range is limited due to the sharpness of the squared Debye loss function.

References and Notes

(1) Böttcher, C. J. F.; Bordewijk, P. *Theory of Electric Polarization*; Elsevier: Amsterdam, 1978; Vol. II.
(2) Cole, K. S.; Cole, R. H. *J. Chem. Phys.* **1941**, *9*, 341–351.
(3) Davidson, D. W.; Cole, R. H. *J. Chem. Phys.* **1950**, *18*, 1417.
(4) Havriliak, S.; Negami, S. *J. Polym. Sci.* **1966**, *C14*, 99–117.
(5) Williams, G.; Watts, D. C. *Trans. Faraday Soc.* **1970**, *66*, 80–85.
(6) Williams, G.; Watts, D. C. *Trans. Faraday Soc.* **1971**, *67*, 1323–1335.
(7) Ngai, K. L. *Comments Solid State Phys.* **1979**, *9*, 127–140.
(8) Schönhals, A.; Schlosser, E. *Colloid Polym. Sci.* **1989**, *267*, 125–132.
(9) Kremer, F.; Schönhals, A.; Schlosser, E. *Phys. Rev. Lett.* **1991**, *67*, 999–1002.
(10) Jonscher, A. K. *Dielectric Relaxation in Solids*; Chelsea Dielectric Press: London, 1982.
(11) Dissado, L. A.; Hill, R. M. *Proc. R. Soc. London, Ser. A* **1983**, *390*, 131–180.
(12) Starkweather, H. W., Jr. *Macromolecules* **1981**, *14*, 1277–1281.
(13) Starkweather, H. W., Jr. *Macromolecules* **1990**, *23*, 328–332.
(14) McCrum, N. G.; Read, B. E.; Williams, G. *Anelastic and Dielectric Effects in Polymeric Solids*; John Wiley & Sons: London, 1967.
(15) Crine, J. P. *IEEE Trans. Electr. Insul.* **1991**, *26*, 811–818.
(16) Bernes, A.; Boyer, R. F.; Lacabanne, C.; Inbar, J. P. In *Order in the Amorphous State of Polymers*; Keinath, S. E., Ed.; Plenum Press: New York, 1987; pp 305–326.
(17) Savitzky, A.; Golay, M. J. E. *Anal. Chem.* **1964**, *36*, 1627–1639.
(18) Gorry, P. A. *Anal. Chem.* **1990**, *62*, 570–573.
(19) Saito, N.; Okano, K.; Iwayanagi, S.; Hideshima, T. *Solid State Physics Advances in Research and Applications*; Seitz, F., Turnbull, D., Eds.; Academic Press: New York, 1963; Vol. 14.
(20) Steeman, P. A. M.; Gondard, C.; Scherrenberg, R. L. *J. Polym. Sci. B: Polym. Phys.* **1994**, *32*, 119–130.
(21) Matsuoka, S.; Quan, X. *Macromolecules* **1991**, *24*, 2770–2779.
(22) Sauer, B. B.; Avakian, P.; Starkweather, H. W., Jr.; Hsiao, B. S. *Macromolecules* **1990**, *23*, 5119–5126.
(23) Starkweather, H. W., Jr. *Macromolecules* **1993**, *26*, 4805–4808.
(24) The choice for the Cole–Cole equation is rather arbitrary and for illustration purposes only (the Cole–Davidson and the Havriliak–Negami equations can be used as well). It does not affect the general applicability of the data evaluation method introduced. However, using a specific analytical equation has the advantage that the denominator and the numerator in eq 16 can be solved both analytically and numerically. This offers the possibility for a double check on the soundness of the fine-structure method and on the accuracy of the calculated derivatives which have to be obtained numerically in analyzing measured data.